J Solid State Electrochem (2011) 15:2199–2204
DOI 10.1007/s10008-010-1229-z

ORIGINAL PAPER

The effect of co-electrodeposited ZrO_2 particles on the microstructure and corrosion resistance of Ni coatings

Reza Arghavanian · Naghi Parvini-Ahmadi

Received: 22 August 2010 / Revised: 16 October 2010 / Accepted: 24 October 2010 / Published online: 16 November 2010

Abstract Pure Ni and Ni–ZrO_2 composite coatings were electroplated using a Watt's bath containing different amounts of ZrO_2 to be co-deposited. Surface morphology and microstructure of the samples and particle distribution in the coatings were studied using optical microscope, scanning electron microscopy, energy-dispersive X-ray spectroscopy, and X-ray diffraction. The results showed that the electroplated sample in the bath containing 90 gl^{-1} ZrO_2 has the maximum particle content and the best particle distribution. Evaluation of microstructure and corrosion behavior demonstrated that with increasing ZrO_2 content in the coating, the corrosion potential shifted toward noble and positive values. This is probably due to diminishing of the metallic surface area exposed to the solution. Higher ZrO_2 contents in the coating results in lower corrosion current densities probably due to the changing of the microstructure from coarse-grained columnar to fine-grained granular structure. The results revealed that the electroplated sample in the bath containing 90 gl^{-1} ZrO_2 has the best corrosion resistance.

Keywords Ni–ZrO_2 composite coatings · Particle distribution · Columnar growth · Granular structure · Corrosion resistance

Introduction

Co-electrodeposition technique is a low-cost and low-temperature method suitable for producing metal matrix composite coatings for diverse purpose such as wear resistance, corrosion resistance, high-temperature corrosion protection, oxidation resistance, self-lubrication, and abrasion resistance. These coatings typically contain oxide particles or carbide particles in micron, submicron and nanosizes such as TiO_2, Al_2O_3, ZrO_2, SiC, etc., in an electrodeposited matrix [1–8].

Nickel is an engineering material which has been widely used as metal matrix [1, 8, 9], and ZrO_2 is an inert particle having many superior properties, such as high melting temperature, low thermal conductivity, and high chemical stability, which are applied in thermal barrier coatings, temperature and flow sensors, superthermal protectors for gas turbines and supersonic propulsion systems of spacecrafts [10–13].

In Ni-ceramic particles composite coatings, ceramic particles played a major role for improving the corrosion protection in two mechanisms. Firstly, these particles act as inert physical barriers to the initiation and development of defect corrosion, modifying the microstructure of the nickel layer and hence improving the corrosion resistance of the coating. Secondly, dispersion of particles in the nickel layer results in the formation of many corrosion microcells in which the particle acts as cathode and nickel metal acts as anode, because the corrosion potential of the particles is more positive than nickel. Such corrosion microcells facilitated the anode polarization. Therefore, in the presence of ceramic particles, localized corrosion is inhibited and mainly homogeneous corrosion occurs [1, 5, 6, 14–17].

Nickel coatings have a high corrosion resistance in many environments and at high temperatures below 875 °C due to form a layer of oxides on the surface of coating. But in a medium containing chloride ion such as seawater (containing NaCl), the ions dissolve the protecting oxide layer in some places and local corrosion cells arise on the nickel surface [17]. Co-deposition of inert particles can inhibit this

R. Arghavanian · N. Parvini-Ahmadi (✉)
Material Faculty, Sahand University of Technology,
Tabriz 53317-11111, Iran
e-mail: parvini@sut.ac.ir

kind of corrosion. ZrO_2 is the selected co-depositing particle. Although Ni–ZrO_2 composite coatings have many applications, some work have been done on the corrosion resistance of these coatings. In this work, microstructure and corrosion resistance of Ni–ZrO_2 composite coatings have been investigated.

Experimental procedures

Pure Ni and Ni–ZrO_2 composite coatings were electroplated using co-electrodeposition method. The electrolyte was Watt's bath of the following composition: 250 gl^{-1} nickel sulfate, 40 gl^{-1} nickel chloride, 45 gl^{-1} boric acid, 50 gl^{-1} sodium citrate, and 0.1 gl^{-1} sodium dodecylsulfate (a wetting agent). Current density was 3 Adm^{-2}, and the bath temperature was maintained at 54±1 °C using a hot plate. The pH of the bath was 3.8–4, and a stirring rate of 200 rpm was provided using a magnetic stirrer. Time of electroplating procedure was 1 h. Samples were cut from St37 steel rod, ground using SiC papers up to 600-grit finish, degreased with 10 wt.% NaOH solution, and pickled in a 30 vol.% HCl solution. Prior to plating, ZrO_2 powder with a particle size of 1–5 μm was dispersed (24 h, 300 rpm) in the bath in amounts ranging from 10 to 130 gl^{-1} in an increasing interval of 20 gl^{-1}. An energy-dispersive X-ray spectroscopy (EDX) system (Oxford) attached to the scanning electron microscopy (SEM) was used to determine the chemical composition of the coatings, and for each sample, five measurements were conducted and the results were averaged. Surface morphologies of the coatings were examined by optical microscope and SEM (Cam Scan model MV2300 operated at 30 kV). X-ray diffraction (XRD) spectra of the samples were obtained using a Bruker D8 Advanced X-ray diffractometer with a Cu Kα radiation (λ=1.5418 Å). The electrochemical studies were performed on a potentiostat/galvanostat device (BHP2063+). The polarization curves of the samples were recorded at a scan rate of 0.01 mVs^{-1} in 3 wt.% NaCl at room temperature. The solution was normally aerated, and the working mild steel electrode soldered with Cu wire for electrical connection embedded in Araldite to offer its cross-sectional area (0.19625 cm^2) in contact with the solution. The measurements were carried out in a three electrodes electrochemical cell with a platinum counterelectrode and a saturated calomel electrode (SCE) as reference. Before experiments, the working electrode was first immersed into the test solution for 2 h to establish a steady-state open-circuit potential.

Stern–Geary equation was employed for calculation of the corrosion current, which is derived as Eq. 1:

$$I_C = \frac{b_a \times b_c}{2.3R_p(b_a + b_c)} \quad (1)$$

where b_a and b_c refer to Tafel constants for the cathodic and anodic reactions, respectively, R_p is the polarization resistance, and I_C is the corrosion current. Surface area fractions were calculated by means of the Clemex image analysis software version 3.5.025.

Results and discussion

Figure 1 shows Zr weight percent of the composite coatings as a function of ZrO_2 concentration in the bath. In constant stirring rate, increasing Zirconia powder content in the electrolyte up to 90 gl^{-1} results in higher amounts of ZrO_2 deposited in the coating. As Zirconia concentration in the electrolyte surpasses 90 gl^{-1}, weight percent of ZrO_2 particles co-deposited in the coating decreases. Extensive error bars for the samples electroplated in the electrolytes containing 110 and 130 gl^{-1} ZrO_2 show that the particle distributions in these coatings are nonuniform.

The SEM micrographs of the samples electroplated in the electrolytes containing 0, 50, 90, and 130 gl^{-1} ZrO_2 (Fig. 2) showed that the sample electroplated in an electrolyte containing 90 gl^{-1} ZrO_2 has the maximum particle content and the best particle distribution in the coating.

Figure 3 shows the XRD patterns for the samples electroplated in the electrolytes containing 0, 50, 90, and 130 gl^{-1} ZrO_2. By increasing ZrO_2 content in the bath up to 130 gl^{-1}, the relative intensity of ZrO_2 diffraction peaks increases and then decreases, showing that the amount of Zirconia in the sample electroplated in an electrolyte containing 90 gl^{-1} ZrO_2 is higher than the other samples.

The relation between powder content in the electrolyte and the amount of particle deposition in the coating depends on the competition between receiving probability of the particles to the surface of the sample and contact probability between particles in the electrolyte. More receiving of the particles to the surface of the sample

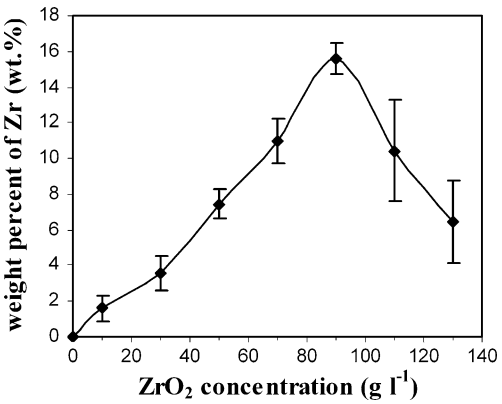

Fig. 1 Weight percent of Zirconium in the coatings versus powder concentration in the bath

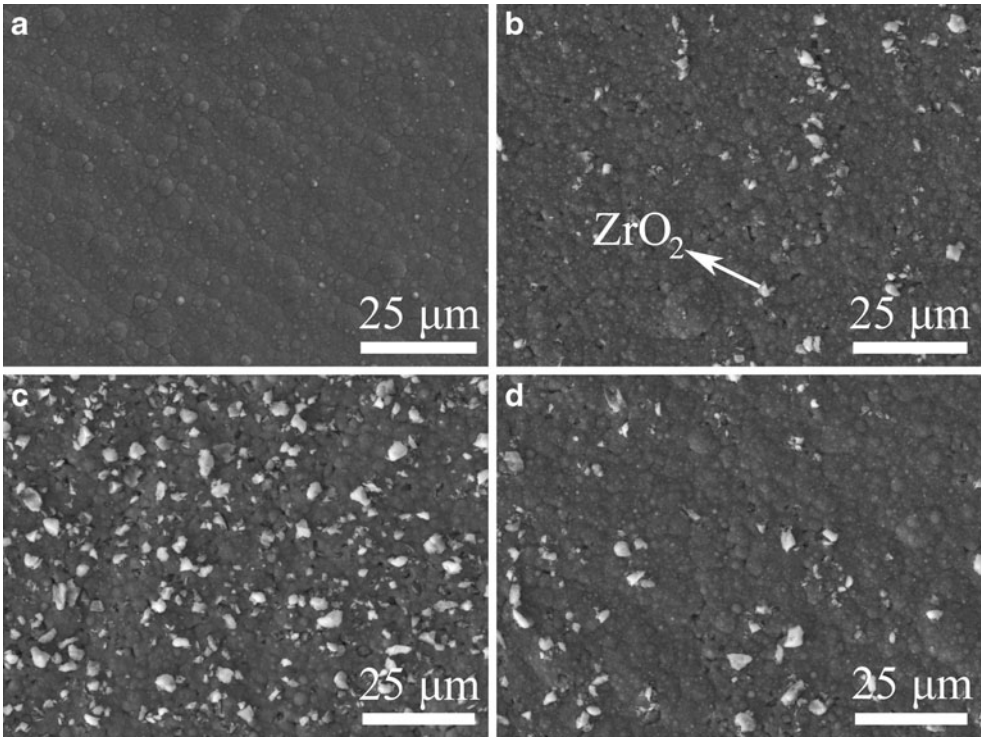

Fig. 2 SEM micrographs of the samples electroplated in the electrolytes containing ZrO_2 concentrations of **a** 0 gl^{-1} (pure Ni coating), **b** 50 gl^{-1}, **c** 90 gl^{-1}, and **d** 130 gl^{-1}

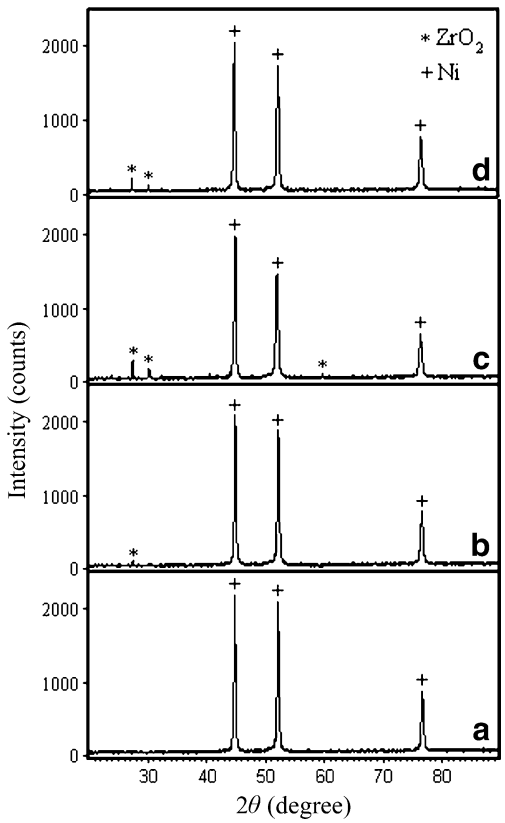

Fig. 3 XRD spectra for the samples which have been electroplated in the electrolytes containing ZrO_2 concentrations of **a** 0 gl^{-1} (pure Ni coating), **b** 50 gl^{-1}, **c** 90 gl^{-1}, and **d** 130 gl^{-1}

results in more co-deposition, but higher contacts between particles in the electrolyte result in higher powder agglomeration and lower co-deposited particles in the coating. Increasing of the powder content in the electrolyte increases both probabilities (receiving and contact), but below 90 g l^{-1}, the receiving probability overcomes the contact probability and the amount of depositing particles in the coating increases. Above 90 gl^{-1}, the contact probability is the predominant factor and the particles co-deposition decreases. On the other hand, more contacts between particles result in nonuniform co-deposition of the particles in the coating.

Figure 4 illustrates typical polarization diagrams for pure Ni coating (sample a) and the sample electroplated in electrolyte containing 90 gl^{-1} ZrO_2 (sample b). The corrosion potential is higher for sample b, indicating more noble corrosion behavior in 3 wt.% NaCl solution.

Figure 5 shows corrosion potential (E_C) plot of the coatings versus ZrO_2 concentration in the bath. Increasing ZrO_2 content in the coating shifts E_C toward positive and noble values (increases E_C), and for the sample electroplated in the bath containing 90 gl^{-1}, ZrO_2, E_C is about 20% higher than pure Ni.

Figure 6 shows surface morphologies of pure Ni coating and the sample electroplated in the bath containing 90 gl^{-1} ZrO_2. Clemex image analysis software showed that about 29% of surface area of sample b is occupied by ZrO_2.

Diminishing of metallic surface area exposed to the solution shifts E_C to more noble and positive values [17].

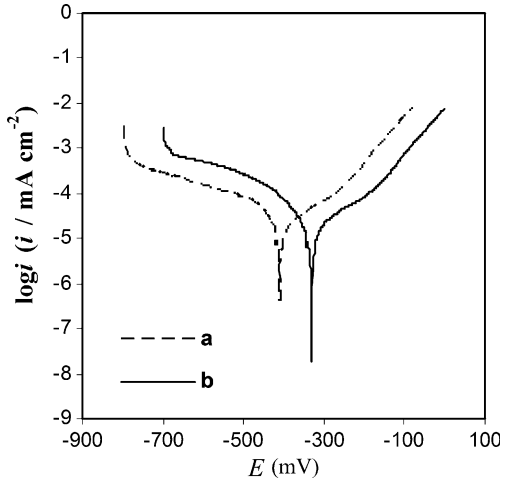

Fig. 4 Polarization diagrams for the samples electroplated in the electrolytes containing ZrO_2 concentrations of **a** 0 gl^{-1} and **b** 90 gl^{-1}

ZrO_2 is an inert particle having high chemical stability, so that in Ni–ZrO_2 composite coatings, the metallic area exposed to the NaCl solution is diminished. This phenomenon probably shifts the corrosion potentials toward more noble and positive values (increases E_C).

Figure 7 illustrates the corrosion current densities (i_C) of the coatings versus ZrO_2 concentration in the bath. Increasing ZrO_2 content in the coating lowers i_C and for the sample electroplated in the bath containing 90 gl^{-1} ZrO_2, i_C is about 50% lower than pure Ni coating.

It can be seen from Fig. 8 that co-deposited particles (ZrO_2) are new nucleation sites for Ni grains. Figure 8a demonstrates SEM micrograph of a Zirconia particle on the surface of the composite coating. Ni nucleus can be seen on the surface of the ZrO_2 particle (arrow 1). In Fig. 8b, cross-section of Ni–ZrO_2 composite coating is shown. Some Ni grains begin from the surface of ZrO_2 particle and nucleation of Ni grains on the surface of ZrO_2 particles is clear (arrow 2).

In Fig. 9, the microstructures of pure Ni coating and Ni–ZrO_2 composite coating have been shown. Ni grains

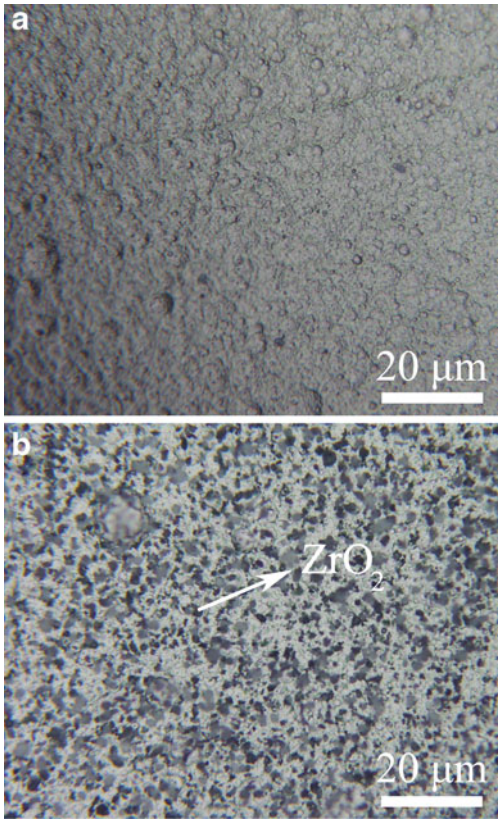

Fig. 6 Optical images of the samples electroplated in the electrolytes containing ZrO_2 concentrations of **a** 0 gl^{-1} (pure Ni coating) and **b** 90 gl^{-1}

(Fig. 9a) have a columnar growth, but the microstructure of composite coating (Fig. 9b) is fine-grained granular due to nucleation and growth of Ni grains on the surface of ZrO_2 particles in various directions. Surface of ZrO_2 particles provide new and appropriate sites for nucleation of Nickel grains (Fig. 8), so that the amount of nucleation sites for Ni grains is higher than pure Ni. Growth rate of Ni grains depends on the conditions of the electroplating procedure, so that growth rates are the same in both samples. Higher

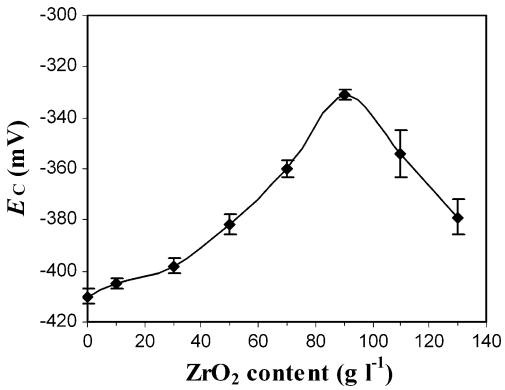

Fig. 5 Corrosion potentials of the coatings versus ZrO_2 concentration in the bath

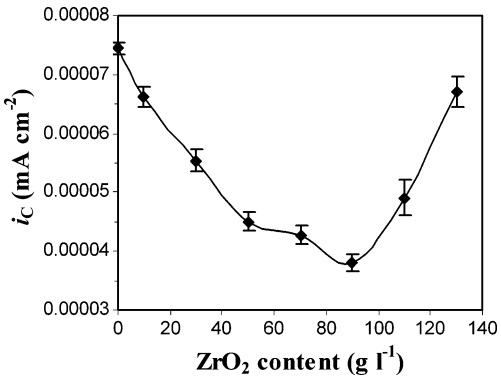

Fig. 7 Corrosion current densities of the coatings versus ZrO_2 concentration in the bath

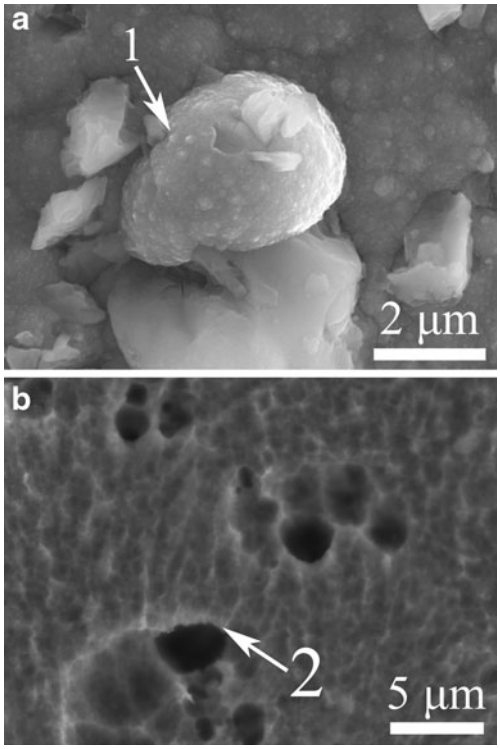

Fig. 8 SEM micrographs of **a** Zirconia particle on the surface of the composite coating and **b** cross-section of Ni–ZrO_2 composite coating (etch: 1 part 10 wt.% NaCN solution + 1 part 10 wt.% $NH_4S_2O_8$ solution)

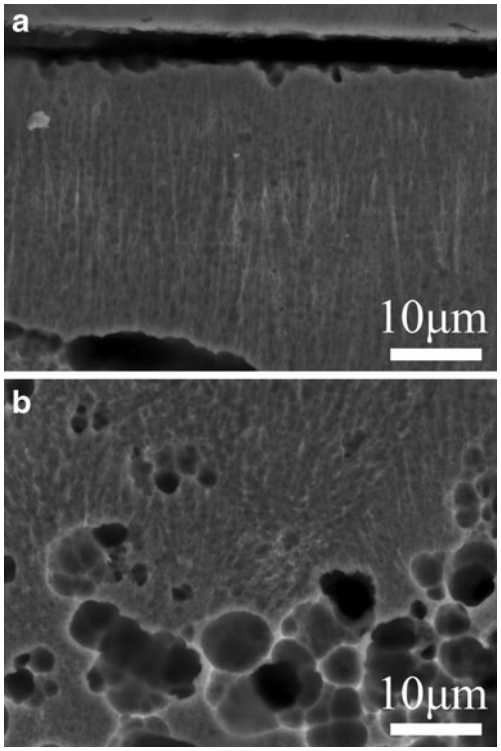

Fig. 9 SEM micrographs of pure Ni (**a**) and Ni–ZrO_2 composite (**b**) coatings cross-sections (etch: 1 part 10 wt.% NaCN solution + 1 part 10 wt.% $NH_4S_2O_8$ solution)

nucleation in constant growth rate results in finer grain size. On the other hand, co-deposited particles (ZrO_2) act as barriers in growth paths of Ni grains and stop the columnar growth of them. In columnar grains (pure Ni grains), the grain boundaries are long and straight (Fig. 9a) from the surface of the coating to the surface of the substrate, but in Ni–ZrO_2 composite coating, Ni grains are spherical-like, so that the grain boundaries become less straight (Fig. 9b).

It was found out that the corrosion process proceeds along the grain boundaries [5, 17]. The long and straight grain boundaries in pure Ni coating are appropriate paths for corrosion proceeding, but in Ni–ZrO_2 composite coating, the grain boundaries are less straight than pure Ni. This changing of corrosion paths from long and straight grain boundaries to less straight paths probably contribute to improved corrosion behavior in Ni–ZrO_2 composite coatings. As much as the particle (ZrO_2) content becomes higher in the coating, the grain boundaries (corrosion paths) become less straight and the corrosion current densities become lower. Increasing of powder content in the electrolyte up to 90 gl^{-1} results in more co-deposition of ZrO2 in the coating and decreasing of i_C. Beyond 90 gl^{-1}, increasing of powder content in the electrolyte results in lower particle content co-deposited in the coating so that grain boundaries become straighter and i_C increases.

Conclusions

1. The amount of ZrO_2 deposited in the coating sharply depends on the bath powder concentration. With increasing of ZrO_2 concentration in the bath up to 90 gl^{-1}, the receiving probability of the particles to the surface of the sample increases so that more ZrO_2 particles co-deposit in the coating. If concentration of ZrO_2 in the bath surpasses 90 gl^{-1}, the contact probability between particles in the electrolyte increases and powder agglomeration occurs so that ZrO_2 content in the coating decreases.
2. Ni–ZrO_2 composite coatings have more noble corrosion potentials than pure Ni. ZrO_2 is an inert particle having high chemical stability. Therefore, in Ni–ZrO_2 composite coatings, the metallic surface area exposed to the NaCl solution is diminished. This diminishing probably shifts the corrosion potentials toward more noble and positive values.
3. Corrosion current densities of Ni–ZrO_2 composite coatings are lower than pure Ni. ZrO_2 particles are new nucleation sites for Ni grains and change structure of nickel from coarse-grained columnar to fine-grained granular structure, so that corrosion can only proceed along less straight paths due to changing of grain boundaries from a long and straight path to a less

straight one. This phenomenon probably lowers the corrosion current densities. Therefore, with increasing ZrO_2 content in the coating corrosion, current density decreases.

4. Maximum amount of ZrO_2 in the coating and the best particle distribution are achieved for electroplated sample in a bath containing 90 gl^{-1} Zirconia powder. Corrosion current density of this sample is about 50% lower, and its corrosion potential is about 20% higher than pure Ni coating.

References

1. Vaezi MR, Sadrnezhaad SK, Nikzad L (2008) Colloids Surf A: Physicochem Eng Asp 315:176–182
2. Zhang H, Qian B (2007) Appl Surf Sci 253:8335–8339
3. Pavlatuo EA, Stroumbouli M, Gyftou P, Spyrellis N (2006) J Appl Electrochem 36:385–394
4. Shrestha NK, Masuko M, Saji T (2003) Wear 254:555–564
5. Garcia I, Conde A, Langelaan G, Fransaer J, Celis JP (2003) Corros Sci 45:1173–1189
6. Hu F, Chan KC, Song SZ, Yang XJ (2007) J Solid State Electrochem 11:745–750
7. Zanella C, Lekka M, Bonora PL (2009) J Appl Electrochem 39:31–38
8. Li YF, Wang YM (2009) Appl Surf Sci 255:4316–4321
9. Bapu GNKR, Jayakrishnan S (2006) Mater Chem Phys 96:321–325
10. Changsong D, Dianlong W, Xinguo H (1997) Surf Coat Technol 91:131–135
11. Sun X, Li S (1998) Surf Coat Technol 105:102–108
12. Leon AB, Rodrıguez AD, Esteban SL, Moya JS, Melendo MJ (2003) J Eur Ceram Soc 23:2849–2856
13. Wen G, Guo ZX, Davies CKL (2000) Scr Mater 43:307–311
14. Benea L, Bonora PL, Borello A, Martelli S, Wenger F, Ponthiaux P, Galland J (2002) Solid State Ion 151:89–95
15. Feng Q, Li T, Teng H, Zhang X, Zhang Y, Liu C, Jin J (2008) Surf Coat Technol 202:4137–4144
16. Abdel Aal A (2008) Mater Sci Eng A 474:181–187
17. Lampke Th, Leopold A, Dietrich D, Alisch G, Wielage B (2006) Surf Coat Technol 201:3510–3517